POLISH MARITIME RESEARCH Special Issue 2018 S2 (98) 2018 Vol. 25; pp. 117-124
10.2478/pomr-2018-0082

NUMERICAL SIMULATION OF SOLID-FLUID 2-PHASE-FLOW OF CUTTING SYSTEM FOR CUTTER SUCTION DREDGERS

Min Zhang, Ph.D.
Shidong Fan, Prof.
Hanhua Zhua, Prof.
Sen Han, Ph.D.
School of Energy and Power Engineering, Wuhan University of Technology

ABSTRACT

The study of the flow characteristics of the solid-fluid two phase flow in the cutter suction dredger is very important for exploring the slurry formation mechanism and optimizing the operational parameters. In this study, standard k-ε model and Multiple Reference Frame are applied to numerically simulate flow field in and around the cutting system, then with the steady convergent result of the simulation as the initial condition, Discrete Phase Mode is used to solve the particle motion equation by fully coupling the continuous phase and the particles . The influence of suction flow velocity and cutter's rotating speed on particles suction are analyzed, and effectively suctioned particles numbers are also quantitatively studied. The simulation result shows that the DPM model is able to simulate the movement of particles in and around the cutter suction dredger's cutting system, in the fluid flow filed velocity vector and pressure distribution on different planes show different characteristics, and under higher suction velocity and lower cutter rotating speed more particles are suctioned into the suction inlet. The results can help better understand flow characteristics of solid-fluid 2-phase-flow of cutter suction dredger's cutting system, and provide theoretical support for relative system design and operational parameters optimization.

Keywords: Numerical Simulation; Solid-Fluid, DPM; Cutting System; Cutter Suction Dredger

INTRODUCTION

Cutter suction dredger is increasingly widely used worldwide for its wide dredging depth range, good soil adaptability and high working efficiency, and it can continuously complete cutting, discharging and slurry treatment processes one time. [1] Flow characteristics of the solid-fluid 2-phase-flow in and around the cutting system of the cutter suction dredger(CSD) depend on several factors including the soil property, the dredger's structural and operational parameters composed of cutter rotational speed, swing speed and pump rotational speed and so on. Investigation on flow characteristics of this solid-fluid 2-phase-flow will be significant for slurry formation mechanism exploring and operational parameters optimization.

The cutting system and slurry transportation system cooperate to cut the soil and discharge the slurry, their respective performance and cooperation level nearly determine the working efficiency of the whole dredger. Particularly for CSD's cutting system, in most working conditions operational parameters are hard to precisely compute and adjust, so the dredger operators are most likely to rely on their experience, the dredger's working efficiency depends on the dredger operator's experience and hardly keeps stable and high. Furthermore, underwater measuring is not only difficult to carry out but also costs much time and investment. So scaled model experiment or computer simulation based on theoretical or prototype model will be more flexible, practical and economic to study the solid-fluid 2-phase-flow for the CSD.

Experimental method generally measures the velocity field with Particle Image Velocimetry (PIV) or other instrument capturing particle trajectory[2]. In computer simulation, CFD models of VOF, Mixture model or turbulence models coupling with Discrete Element Method(DEM) have been applied to handle solid-fluid 2-phase-flow. Some scholars have applied the discrete phase model (DPM) to simulate the flow characteristics of two-phase-flow for cyclone separator, centrifugal pump, complex pipeline and ballast water cyclone[3-6]. For CSD's cutting system, fluid flow simulation based on turbulence models has been studied [7, 8]. Research on simulation of 2-phase-flow of CSD's cutting system is relatively rarely focused.

In this paper, standard *k-ε*, MRF and DPM models are applied to simulate the solid-fluid 2-phase-flow of CSD's cutting system, and influence of suction velocities and cutter rotating speeds on suctioned particles is also analyzed.

GEOMETRIC AND MATHEMATICAL MODELS

GEOMETRIC MODEL AND BOUNDARY CONDITIONS

Computational domain is set with 14m in swing direction, 8.5 m in vertical and 7.5m in horizon. Ladder angle is 35 degrees as cutter's dredging position. The 3-dimensional geometry model and computational domain is shown as Fig. 2. The particle source location, where slurry particles produces, is simplified to be the inner side of 2 cutting cutter arms as shown in Fig. 1, and the slurry particles are treated as spherical.

In order to monitor the internal pressure and velocity inside the suction inlet, five sampled points marked with L1-L5, located on the plane parallel to the cutter ring and with the same radius to the cutter hub center, are taken as shown in Fig. 1.

The computational domain is meshed with structured and unstructured meshes, after simulation testing when mesh number is over 1.38 millions, the increase of mesh number has little effect on the accuracy of the calculation results. So mesh number of 1.38 millions is taken in the simulation.

The inlet of the computational domain is set velocity inlet with typical value of 0.2m/s to simulate cutting system swing movement. Suction inlet of cutting system is set to velocity type with adjustable flow rate between 1.5m/s–4m/s, which is one of the computational outlets. The bottom of the computational domain is set as wall type. In addition to the inlet and the bottom, the other sides of the whole computational domain are set pressure outflow. The rotating speed of the rotating domain can be set 15 rpm to 70 rpm with the axis of the cutter hub as rotating hub. Walls of cutter, hub, and backplate are set non-slippery boundaries. And the injected particles' diameters range from 1mm to 5mm. Boundary conditions of inlet and outlet for particles are taken as escaped or trapped. The type of collision between the particle and the cutting system body boundaries is set as elastic rebound.

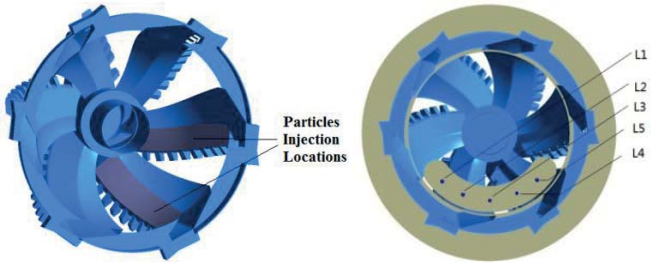

Fig. 1. Targeted Locations in Cutter Flow Field

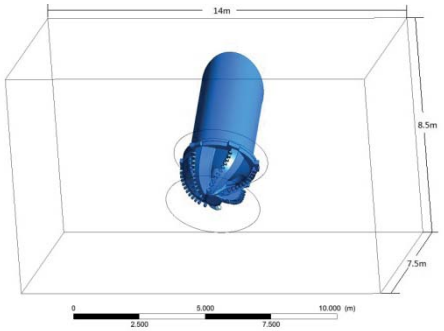

Fig. 2. Computing Domain of Cutting System Flow Field

MATHEMATICAL MODEL

In this study, water is treated as the continuous and incompressible fluid, so its governing equations are mass and momentum conservation equations. The Reynolds Averaged N-S equation is adopted to describe the fluid.

Mass conservation equation is as Eq. (1),

$$\frac{\partial \rho}{\partial t}+\frac{\partial}{\partial x_i}(\rho u_i)= \tag{1}$$

Momentum conservation equation is as Eq. (2),

$$\rho\frac{\partial u_i}{\partial t}+\rho u_j\frac{\partial u_i}{\partial u_j}=pF_i-\frac{\partial p}{\partial x_i}+\frac{\partial}{x_j}(\mu\frac{\partial u_i}{\partial x_j}-\rho\overline{u_i'u_j'}) \tag{2}$$

In Eq. (1) and Eq. (2), u_i is liquid velocity in direction x, p is liquid pressure, μ is kinetic viscosity, is fluid mass force, $\rho\overline{u_i'u_j'}$ is Reynolds Stress. The Reynolds equation is closed by the standard k-ε mode[9,10]in which turbulent kinetic energy equation is Eq. (3) and turbulent diffusion equation is Eq. (4).

$$\frac{\partial}{\partial t}(\rho k)+\frac{\partial}{\partial x_i}(\rho k u_i)=\frac{\partial}{\partial x_j}\left[\left(\mu+\frac{\mu_t}{\sigma_k}\right)\frac{\partial k}{\partial x_j}\right]+G_k+G_b-\rho\varepsilon-Y_M+S_k \tag{3}$$

$$\frac{\partial}{\partial t}(\rho\varepsilon)+\frac{\partial}{\partial x_i}(\rho\varepsilon u_i)=\frac{\partial}{\partial x_j}\left[\left(\mu+\frac{\mu_t}{\sigma_\varepsilon}\right)\frac{\partial \varepsilon}{\partial x_j}\right]+C_{1\varepsilon}\frac{\varepsilon}{k}(G_k+C_{3\varepsilon}G_b)-C_{2\varepsilon}\rho\frac{\varepsilon^2}{k}+S_\varepsilon \quad (4)$$

$C_{1\varepsilon}$, $C_{2\varepsilon}$, $C_{3\varepsilon}$ are coefficients of constant terms of the equation,

G_k, G_b are the velocity gradient and the turbulent kinetic energy generated by the buoyancy respectively,

S_k, S_ε are user-defined functions,

G_k is the fluctuation of the pulsation expansion,

$\mu=\rho C_u\frac{k^2}{\varepsilon}$ is turbulence viscosity coefficient.

In the solid-fluid two-phase-flow field, the forces acting on a single particle are gravity, buoyancy, flow resistance, additional mass force, pressure gradient force, Basset force, Saffman lift force, Magnus force and so on [11,12]. For the particle size this study concerns, gravity, buoyancy, drag force, added mass force, pressure gradient force and forces related to rotation movement are focused. The force balance equation of the particles can be expressed as Eq. (5) in the Cartesian coordinate system,

$$m_p\frac{dU_p}{dt}=G_p+F_b+F_d+F_{VM}+F_p+F_{BA}+F_R \quad (5)$$

The particle gravity and buoyancy acting by the fluid can be described as Eq. (6),

$$G_p+F_b=m_p\cdot g\cdot(1-\frac{\rho_f}{\rho_p}) \quad (6)$$

The drag force acting on particle is as Eq. (7),

$$F_D=\frac{18\mu}{\rho_p d_p}\cdot\frac{C_d R_{ep}}{24}(u_f-u_p) \quad (7)$$

$$F_d=mF_D=\frac{\pi\mu d_p C_d R_{ep}}{8}(u_f-u_p) \quad (8)$$

$$R_{ep}=\frac{\rho_d d_p}{\mu}\left|u_p\text{-}u_f\right| \quad (9)$$

In Eq. (7), is particle density, F_D is the drag force of unit mass particle, is particle diameter, is drag coefficient, is particle Reynolds number, the flow velocity of particle's location, and is particle velocity.

Particles will drive a certain amount of surrounding fluid to move together in fluid motion. When the particle is accelerating, the surrounding fluid will be accelerated as a result of particle driving effect, which can be equivalent to particle mass increase. The particle's virtual mass force F_{vm} is expressed by Eq. (10) and Eq. (11),

$$F_{vm}=K_m\rho_f V_p\left(\frac{du_f}{dt}-\frac{du_p}{dt}\right) \quad (10)$$

$$K_m=1.05-\frac{0.066}{A_c^2+1.02} \quad (11)$$

A_c is particle acceleration modulus.

$$F_p=-\frac{\pi d_p^3}{6}\cdot\nabla p \quad (12)$$

F_p is the pressure difference force acting on the particles.

In the process of particle movement, the velocity is variable, fluid displacement force is acting on the particle due to the instability of surface boundary layer. For the particle with diameter between 1-5mm, the influence of Basset force can't be neglected by magnitude analysis [13] .

$$F_{BA}=\frac{3d_p^2}{2}\sqrt{\pi\mu\rho_f}\int_{t_0}^{t_1}\frac{\frac{d\mu_f}{dt}-\frac{d\mu_p}{dt}}{\sqrt{t-t'}}dt' \quad (13)$$

The cutter is rotating during dredging, and the particles are also acted by the centrifugal force and Coriolis force. If the cutter axis is set as the Z axis, the geometric center of cutter-ring's bottom plate is set as Cartesian coordinate origin, forces acting on the unit mass particle related to cutter rotating movement can be expressed in Cartesian coordinate system as Eq. (14),

$$\begin{cases}\mathrm{F}_{\Omega,x}=(1-\frac{\rho_f}{\rho_p})\cdot\Omega^2\cdot x+2\Omega(\mathrm{u}_{y,p}-\frac{\rho_f}{\rho_p}\mathrm{u}_{y,p})\\ \mathrm{F}_{\Omega,y}=(1-\frac{\rho_f}{\rho_p})\cdot\Omega^2\cdot y+2\Omega(\mathrm{u}_{x,p}-\frac{\rho_f}{\rho_p}\mathrm{u}_{x,p})\end{cases} \quad (14)$$

The velocity and trajectory of each position on the discrete phase can be solved by integrating the differential equation of particle force in the Laplace coordinate system.

The governing equations are converted into algebraic equations which can be solved numerically by finite volume method with pressure-based solver. In the simulation pressure equations coupling method is chosen. The pressure term is adopted in the PRESTO format, the momentum, the turbulent kinetic energy and the turbulent dissipation rate are all set as the high accuracy two order upwind scheme. The convergence judge for all variables is that the residual value is less than 10^{-3}.

MULTI-REFERENCE FRAME MODEL

In order to simulate the rotation of the cutter, Multiple Reference Frame (MRF) is adopted. The computational domain is divided into rotating domain and stationary domain. The rotating coordinate system in rotating cylindrical domain

is set as local system and the fixed coordinate system in stationary domain is regarded as absolute coordinate system. The coupling between the rotating zone and the stationary zone is realized through interface of the two domains, and finally the bidirectional continuous transfer of mass and energy between the two reference frames are realized by interfaces in MRF model[14]. Velocity and velocity gradients can be converted from reference frame to absolute inertial frame by interface between the rotor and stator defined in Fluent.

ANALYSIS OF SOLID-FLUID 2-PHASE-FLOW OF CUTTING SYSTEM

VELOCITY VECTOR AND PRESSURE ANALYSIS OF FLUID PHASE

The simulation is carried out based on the standard k-ε model in steady state with typical operational parameters (cutter rotating speed is 30rpm, suction velocity of the suction inlet is 2.0m/s and swing speed is 0.2m/s). 4 planes with heights of 0m, 0.45m, 0.7m, 1.6m, from the surface of cutter ring top plate and perpendicular to the cutter hub axis are sampled. The cutter radial velocity vector diagrams in rotating region (absolute velocity vector diagram, the global coordinate system as the reference) are shown in Fig. 3.

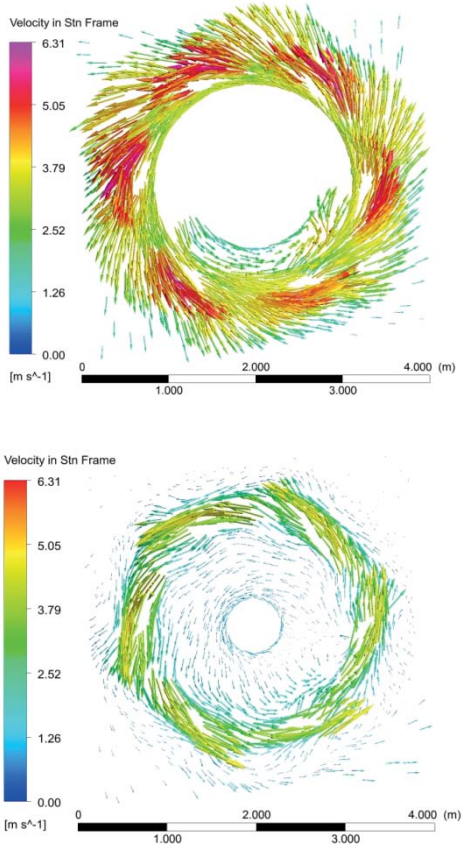

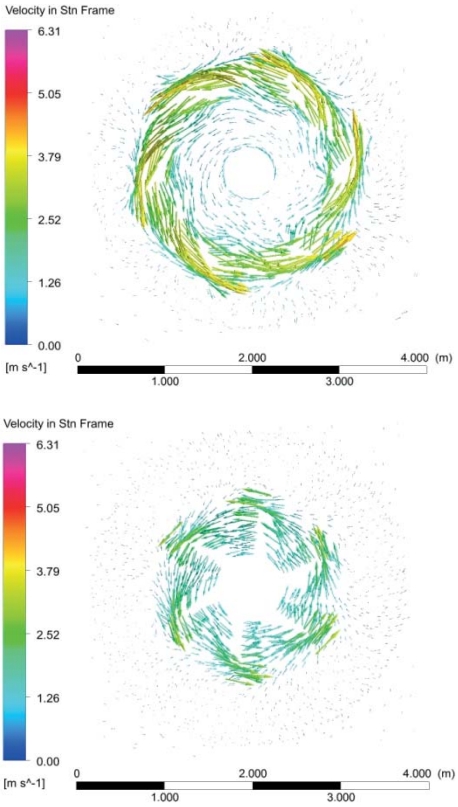

Fig. 3. Velocity Vector Diagram of Sample Planes

From Fig. 3, the rotating region full of rotating fluid forms a large vortex around cutter hub, and the vortex dominates the fluid flow in and around the cutting system, because the cutter drives the fluid in the domain in the tangential direction. On the other hand, suction effect due to suction inlet defers in different sampled planes. Near the cutter ring top (h=0m) rotating effect is greater than the suction effect, fluid excluding fluid inside the suction inlet is nearly unaffected by the suction effect, and a large number of fluid particles are thrown out of the cutter. On the plane of h=0.45, fluid particles flow across the cutter arm to the suction flow direction with high axial velocity as a result of suction inlet's suction and cutter rotating. Part fluid particles in the rotating domain flow into inner part of the cutter from opening of adjacent cutter arms, and some of those rotate with cutter hub and finally reach approach of the suction inlet, the others flow directly to the suction inlet direction. On the plane of h=0.70m, fluid motion characteristics are similar to those of h=0.45m, but the cutter radius is smaller in h=0.70m so fluid tangential velocity becomes smaller. On the planes of h=0.70m and h=1.6m, the suction effect is more weakened in turn, and affected by the hub occupation and smaller cutter opening, fluid particles have axial velocity, but the movement trend to the suction inlet is not obvious. Furthermore, with further decrease of the cutter radius, tangential velocity further decreases accordingly.

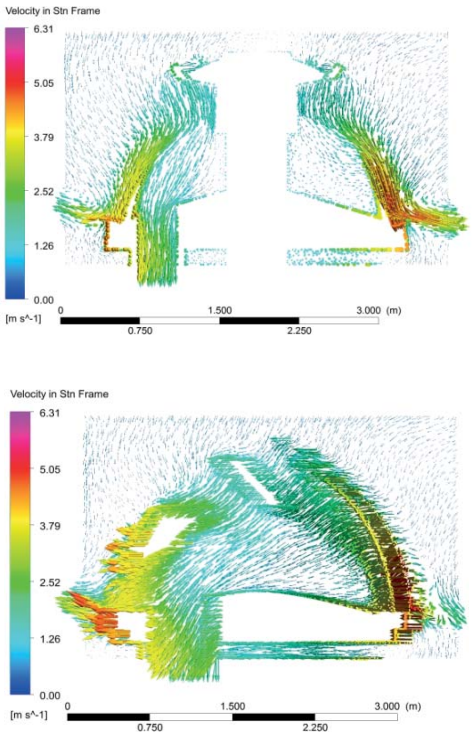

Fig. 4. Velocity Vector Diagram of Sample Planes

In order to analyze the fluid velocity vector of the planes perpendicular to the cutter ring top surface, two planes are selected which are located on the central plane(z=0) and the plane with distance of 0.6m from the central plane and parallel to the sampling plane of z=0. From velocity vector diagram of the central plane, it can be found that much fluid is approaching or entering the suction inlet due to the pump suction. With the pumping effect, macroscopic moving trend of the fluid is approaching toward the inside of the cutter through cutter arms openings, some fluid particles are rotating outside of the cutter for they are hold back by the cutter arms, and the longer the fluid particle location's radius is the higher its velocity is, most fluid particles near the cutter ring are thrown out. For fluid particles within the cutter, the velocities of fluid particles in the suction inlet side has a greater velocity component in cutter axis direction than components in cutter radial plane, most fluid particles on the opposite side of the suction inlet within the cutter keep rotating instead of approaching the suction inlet. On the plane of 0.6m from the hub, outside the cutter much fluid particles are approaching the cutter inside from openings of the cutter arms, in the cutter all fluids are trending to entering the suction inlet.

Under above cutting operating conditions, cutter radial plane's static pressure (relative pressure, the reference pressure is atmospheric pressure with 101Kp) contours are shown in Fig. 5, sampled planes are the same with velocity vector diagrams of Fig. 3..

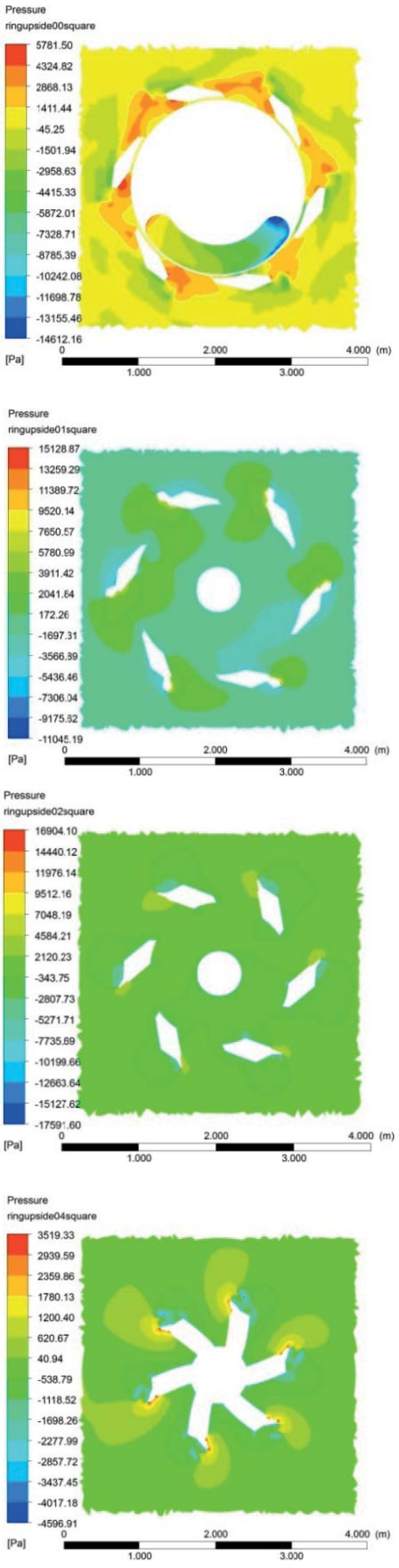

Fig. 5. Radial Pressure Contours

From the pressure contour of the plane of h=0m, in the suction inlet the pressure of the right region is less than that of the left, and the reason is that when the fluid particles are approaching to the suction inlet in a spiral way velocity increases and the pressure decreases, and the cutting system's geometry leads to the uneven pressure distribution, part fluid of the left is blocked and its pressure is greater than that of the right. On the pressure contours of the planes of h=0.45m, 0.7m, the pressure in the outer region of each cutter arm increases, this is because the fluid flows toward the suction inlet by pump suction effect and collides with cutter arm leading to velocity decrease as well as the pressure rise, so the cutter arm strength of these positions should be especially strengthened. On the planes of h=0.45m, 0.7m, pressure of the region near the suction inlet in the cutter is relatively lower for the velocity increases and the pressure decreases because of suction effect of suction inlet. And on the plane of h=1.6m a slightly high pressure region near the outer side of the cutter can be observed, and the reason lies in that some fluid particles strike the arm leading to velocity decrease and pressure increase.

PARTICLE TRAJECTORY ANALYSIS

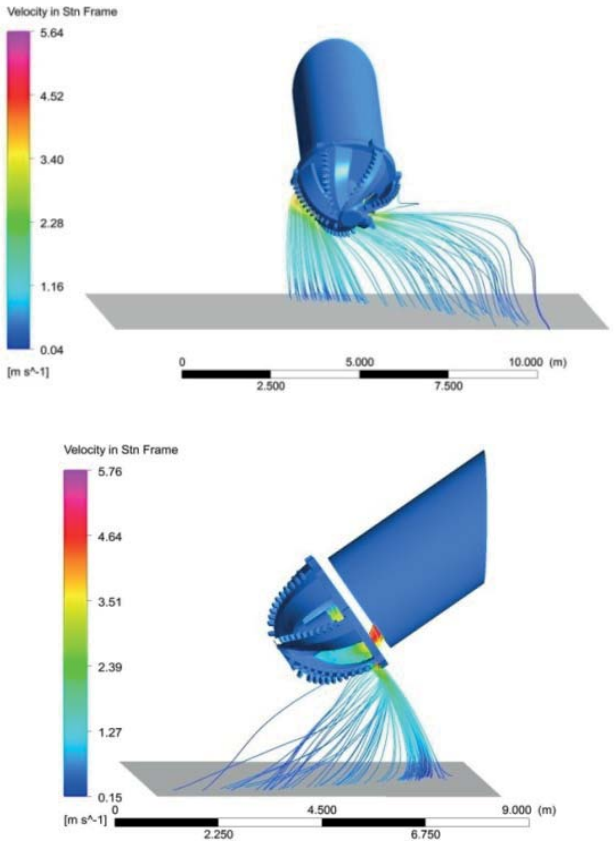

Fig.6. Particle Trajectory Colored by Velocity

Under the simulating operational conditions some of the dredged particles are approaching and entering the suction inlet, while the others are rotating outward of the cutter and captured by the computing domain boundaries. The residential time and diameter distribution of the source particles can be tracked based on DPM model. From Fig. 6, it can be observed the number and residence time of particles depend on the cutter speeds and the inlet suction velocity. The velocities of the particles near the cutter outside and in the suction pipe are higher than those of other places.

INFLUENCE ANALYSIS OF OPERATIONAL PARAMETERS

SUCTION VELOCITY INFLUENCE ON SUCTION EFFICIENCY

With the same cutter rotation speed and swing speed the solid-fluid 2-phase-flow with suction flow velocities of 1.5m/s, 2.0m/s, 2.5m/s, 3.0m/s, 3.5m/s is simulated and compared. The variations of velocity at L1-L5 in suction inlet channel under different suction velocities are shown in Fig. 7. It demonstrates that under the same cutter rotation speed and swing speed, increasing suction flow velocity will result in nearly linear increase of the sampled locations' velocities. For suction velocity is directly determined by the pump driving power, and the pump energy consumption accounts for a large proportion of the total energy consumption during dredging, so setting a reasonable suction velocity should balance the pumping effect and the energy consumption.

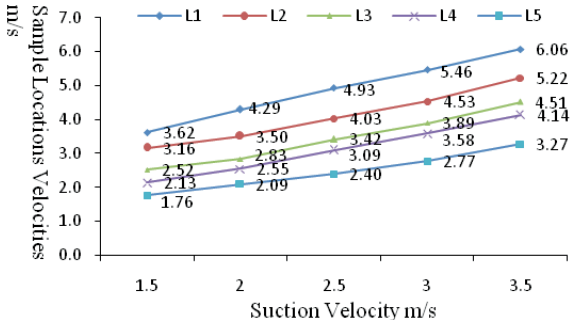

Fig. 7. Velocities of Sample Points under Different Suction Velocities

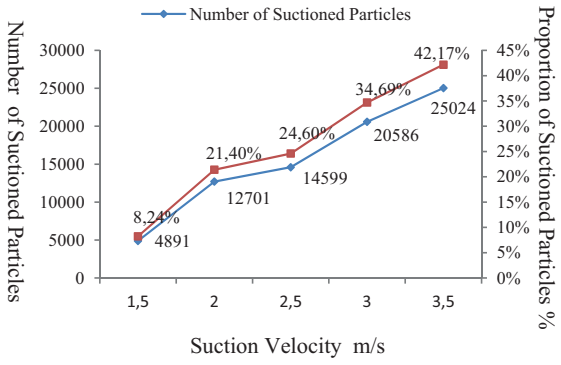

Fig. 8. Suctioned Particles Numbers with Different Suction Velocities

In this study, the number and the proportion of the suctioned particles per unit time are calculated to analyze the suction characteristics influence to the suction efficiency. Fig. 8 shows that the higher the suction flow velocity is, the more influence of the pressure difference force has and the higher the suction efficiency is.

CUTTER ROTATING SPEED INFLUENCE ON THE SUCTUION EFFICENCY

The number and the proportion of the suctioned particles per unit time are counted to analyze the cutter rotating speed influence to the suction efficiency. Fig. 8 shows that the higher the cutter rotating speed is, the greater influence of the particle's centrifugal movement is, and the lower efficiency the cutting system reaches. But when cutter rotating speed is up to 60 rpm, part particles rotate around and cross the hub and arrive the suction inlet, so the suctioned particles is 0.78% more than those of 50 rpm.

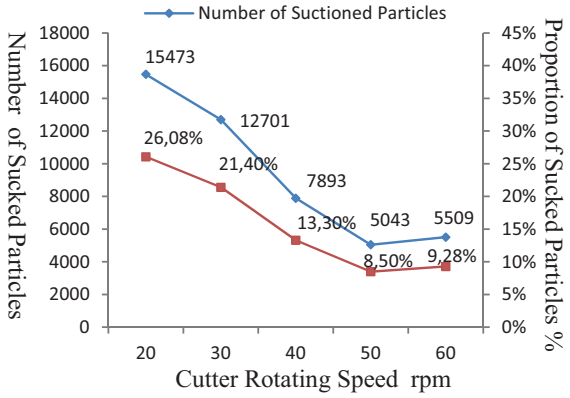

Fig. 8. Suctioned Particles Numbers with Different Cutter Rotating Speeds

CONCLUSIONS

With typical cutter rotating speeds, swing speeds and suction velocities, standard k-ε model and Multiple Reference Frame model are introduced to simulate the fluid flow field of the cutting system for the cutter suction dredger. Then DPM model is applied to compute the solid phase movement equation by two-way coupling interaction between particles and fluid. The main conclusions are drawn as follows:

(1) in condition of low concentration of the solid phase, the DPM model is able to simulate the particle trajectory for cutting system of CSD.
(2) in the fluid flow filed velocity vector and pressure distribution on different planes show different characteristics.
(3) the suction velocity of the suction inlet and the cutter rotating speeds have great influence on the flow field characteristics of cutting system of the CSD, higher suction velocity and lower cutter rotating speed will suction more particles into the suction inlet.

ACKNOWLEDGMENT

The research has been supported by the National Natural Science Foundation of China (No. 51179144 and No. 51679178).

BIBLIOGRAPHY

1. Tang Jianzhong: Research on Optimization and Control of Dredging Operations for Cutter Suction Dredgers. Hangzhou: Zhejiang University, pp.1-3, 2007
2. Yaling Li, Shouqi Yuan, Yue Tang, Ping Huang, Xiaojun Li: Discrete Phase Model Simulation of Tracer Particle Motion in Centrifugal Pump. Chinese Journal of Agricultural Machinery, Vo.l43, no.11, pp.113-115, 2012
3. Li Dan, Ma Guiyang, Du Mingjun, Wang Haifeng: Numerical Simulation for Particles Track in a Cyclone Separator Based on the DPM. Journal of Liaoning Shihua University, Vol. 31, no.2, pp.37-38, 2011
4. Liu Juan, Xu Hongyuan, Tang Shu, Lu Li: Numerical Simulation of Erosion and Particle Motion Trajectory in Centrifugal Pump. Chinese Journal of Agricultural Machinery, Vol. 6, no. 2, pp.54-59, 2008
5. Zhang Tao, Li Hongwen: Simulation Optimization of DPM on Gas-Solid Two-Phase Flow in Complex Pipeline Flow Field. Journal of Tianjin Unversity (Science and Technology). Vol.48, no. 1, pp.39-46, 2015
6. Xu Yanxia, Song Xingfu, Tang Bo, Wang Jin, Yu Jianguo: Analysis Structural Parameters of Hydrocyclone used in Ballast Water on its Performances. Chemical Industry and Engineering Progress. Vol.36, Sup. 2, pp.81-85, 2016
7. M. A. Dekker, N. P. Kruyt, M. den Burger, W. J. Vlasblom: Experimental and Numerical Investigation of Cutter Head Dredging Flow. Journal of Waterway, Port, Coastal and Ocean Engineering. Vol. 129, no 5, pp.203-209, 2003
8. Fang Yuan, Ni Fusheng: Numerical Simulation of 2-D Water Flow in and around Cutter of a Dredger. China Harbour Engineering. Vol. 173, no. 2, pp.4-5, 2011
9. Marzio Piller, Enrico Nobile, Thomas. J: DNS Study of Turbulent Transport at Low Prandtl Numbers in a Channel Flow. Journal of Fluent Mechanics,Vol.458, pp.419-441, 2002
10. Min Zhang, Shidong Fan, Haoyu Zhang: Flow Field Analysis of Cutter Head for Cutter Suction Dredgers. Proceedings of 2016 International Conference on Human-centered Computing, Sri Lanka, pp.578-579, 2016
11. Xia Mi, Li Yi, Li Fengqin: Numerical Simulation of Solid Phase Movement and Distribution in the Solid-liquid Two

Phase Flow Centrifugal Pump. Journal of Mechanical and Electrical Engineering. Vol. 32, no. 12 ,pp.1555-1557, 2015

12. Vakamalla Teja Reddy, Vadlakonda Balraju, Aketi V. Asha Kumari, Mangadoddy Narasimha: Multiphase CFD Modeling of Mineral Separators Performance: Validation Against Tomography Data. Transactions of the Indian Institute Of Met-als.Vol.70, no.2 ,pp.323-340, 2016

13. Yi Li: The Research on Numerical Simulation and Abrasion Property of Solid-liquid Two-phase-flow Centrifugal Pump. Hangzhou: Zhejiang Sci-tech University, pp.20-21, 2014

14. Zhang Tao, Yang Chenjun, Song Baowei: Investigations on the Numerical Simulation Method for the Open-water Performance of Contra-rotating Propellers based on the MRF Model. Journal of Ship Mechanics. Vol. 14, no. 8, pp.848-849, 2010

CONTACT WITH THE AUTHORS

Shidong Fan, Professor, Ph.D.
e-mail: fsd1963@263.net

Min Zhang, Ph.D.
e-mail: zhm@whut.edu.cn

School of Energy and Power Engineering
Wuhan University of Technology
Heping Avenue No 1178
Wuhan 430063, Hubei
China